Microbiology, Metabolites and Biotechnology
MMB
The former ARMMT

Optimization of L-asparaginase type II produced by *Bacillus velezensis* SE114

Fereshteh Hozoorbakhsh[1], Mozhgan Ghiasian[1]*, Fereshte Ghandehari[1], Zarrindokht Emami-Karvani[1], Maryam Khademi Dehkordi[2]

[1]Department of Microbiology, Falavarjan Branch, Islamic Azad University, Isfahan, Iran
[2]Department of Biology, Falavarjan Branch, Islamic Azad University, Isfahan, Iran
*Corresponding Author: Mozhgan Ghiasian

Article Info

Document Type:
Research Paper

Received 29/10/2023

Scentific Acceptation
21/12/2023
Final Acceptation
30/01/2024
Published 12/05/2024

Keywords:
L-Asparaginase,
Bacillus velezensis,
Optimization,
Response Surface Methodology,
Central Composite Design

Abstract

Once the acute lymphoblastic leukemia cells that need L-asparagine are exposed to L-ASNase, they die because of the limitations of L-asparagine. The globally rising rate of ALL also requires extraordinary efforts to discover new microorganisms with high L-ASNase production and efficiency. The aim of this study is the high amount of L-ASNase production. After isolation, the L-ASNase production was optimized using the response surface methodology and the central composite design. Then, *in-silico* studies were predicted for the L-ASNase-producing gene. In this study, *Bacillus velezensis* was isolated as an L-ASNase producer from slaughterhouse effluent using the M9 medium. The optimization process further illustrated Tween 20, glucose, temperature, and L-asparagine, which were more significant for L-ASNase production. Based on statistical prediction by response surface methodology, more enzyme activity (7.11 U/mL) could be realized at 0.6% Tween 20, 1.7% glucose, 55°C temperature, and 1.8% L-asparagine. The *in-silico* studies also established that the binding site is located at the N-terminal domain and the active site flexible loop. Additionally, it contained Thr36, Ala47, Tyr50, Glu84, Asp117, Thr116, Met142, Lys189, Thr193, and Thr192 as the conserved and functional residues in L-ASNase. It was concluded that *B. velezensis* SE114 produced L-ASNase type II in the present study. The statistical optimization results also showed that Tween 20, glucose, temperature, and L-asparagine were significant variables affecting the L-ASNase production. In addition, temperature and L-asparagine had noteworthy interactions.

1. Introduction

Thanks to its immeasurably useful medical applications, L-asparaginase (L-ASNase, viz., L-asparagine aminohydrolase, E.C.3.5.1.1) has been investigated by many researchers throughout the world. L-asparaginase is utilized in the treatment of different cancers, such as lymphoma, gastric cancer, Lewis lung carcinoma (LLC), breast cancer, ovarian cancer, liver cancer, colorectal cancer, osteosarcoma, and acute myeloid leukemia (AML). It is known as an effective antineoplastic agent; however, since these cells cannot synthesize L-asparagine, L-asparagine is

*Corresponding author. Mozhgan Ghiasian. Department of Microbiology, Falavarjan Branch, Islamic Azad University, Isfahan, E-mail address: mozhgan.ghiasian@iau.ac.ir
DOI: 10.22104/MMB.2023.6391.1115
Please cite this article as: mozhgan. ghiasian, Microbiology, Metabolites and Biotechnology (MMB), https:// DOI: 10.22104/MMB.2023.6391.1115

converted into L-aspartic acid and then releases ammonia (NH_3) because all anticancer drugs need an extracellular source of this amino acid (Darvishi *et al*., 2022).

Although numerous production and purification techniques have been developed for this purpose thus far, they have provided an insufficient quantity of enzymes for limited trials. Accordingly, enzyme production by other microorganisms should be explored. The variables affecting the increase in enzyme production can be surveyed by statistical modeling. Of note, no specified medium exists for the optimized production of L-ASNase in different microorganisms. Additionally, the composition of the fermentation medium and the culture conditions play a profound role in enzyme production, and the production itself is influenced by the numerous interactions of nutritional and environmental factors (Mangamuri *et al*., 2017).

There is little information about the statistical optimization of the L-ASNase production by *Bacillus velezensis*. For this purpose, the screening and evaluation of the nutritional and environmental requirements of a microorganism are among the important stages of developing and determining the overall economic feasibility of bioprocesses (Venil *et al*., 2009). Response surface methodology (RSM) is thus a robust tool for the optimization of experimental conditions in biotechnology since it can evaluate the effect of variables and their interactions in response (Erva *et al*., 2018). In this respect, *B. velezensis* was introduced as an aerobic gram-positive bacillus with endospores (Rabbee *et al*., 2019). It was further isolated as an L-ASNase-producing bacteria from ruined pomegranate on an M9 medium because it is a pathogen for this fruit (Parmar *et al*., 2021). Moreover, it is reported that *B. velezensis* isolated from Red Sea sediment samples using the M9 medium and millipore membrane filtration method can produce L-ASNase without glutaminase (Mostafa *et al*. 2019). The yield of L-asparaginase production obtained under optimized conditions was also compared among *Bacillus polymyxa*, *Bacillus firmus*, *Bacillus velezensis*, and *Bacillus licheniformis*, with results showing the optimum L-asparaginase production was 7.037 U/mL, 5.368 U/mL, 14.03 U/mL, and 36.08 U/mL, respectively (Rahnamay Roodposhti *et al*., 2015).

Against this background, the present study aimed to achieve the optimal conditions for more L-ASNase production from *B. velezensis* using the RSM and the CCD. In this way, the most significant factors, such as pH, incubation time, and carbon and nitrogen sources, were evaluated in the optimization. Furthermore, an *in-silico* analysis of the L-ASNase sequence was performed, and the three-dimensional (3-D) structural model was evaluated to delineate the functional structure and the binding site residues of the protein.

2. Materials and Methods

2.1. Microorganism

To meet the study objectives, several strains of bacteria were isolated from the effluent and soil samples from a slaughterhouse in Esfahan, Iran. To screen the L-ASNase-producing bacteria, an M9 medium was prepared without Tween 20. Then, the pH was adjusted to 6.8. Two media without the indicator (phenol red [phenolsulfonphthalein or PSP]) and L-asparagine (including sodium nitrate [$NaNO_3$]) were used as the negative control medium (Mohammadi-Sichani *et al*., 2019). The L-ASNase-producing bacteria were then isolated by changing the color of the M9 medium into pink by hydrolyzing L-asparagine to ammonium (NH_4^+), creating an alkaline environment.

2.2. Analysis of 16S Ribosomal Ribonucleic Acid (16SrRNA) Sequence

Marmur's manual method was used to extract the genomic deoxyribonucleic acid (DNA) of the selected isolate (Ghiasian *et al*., 2017). The phylogenetic analysis of the 16SrRNA gene was used for molecular identification. The 16SrRNA gene (530 bp fragment) was thus amplified using the PCR technique together with two universal primers (R518 and F8, Sinaclon, Iran), and

sequencing was completed at Macrogen (Seoul, South Korea). The results were then evaluated in terms of homology and similarity using Chromas Lite version 2.1 and the BLAST Tool (Basic Local Alignment Search) at the National Center for Biotechnology Information (NCBI) database.

2.3. Sequence Retrieval

The L-ASNase gene fragment was here amplified by the PCR technique (primary temperature: 94°C (5 minutes), 10 cycles: 94°C (30 seconds), 55°C (30 seconds), 72°C (55 seconds), 25 cycles: 94°C (30 seconds), 52°C (30 seconds), and 72°C (55 seconds), 35 cycles: 5°C (5 minutes)). Two primers, FBVaspFH (AAACAATTCATGCCCTTCATTAC) and RBVaspFH (GTACTCATTGAAATAGGTTTGAATC), were used for amplification. PCR products were also determined by Macrogen (Seoul, South Korea). The sequence was further analyzed using the Chromas Lite (version 2.1) and the CAP3 tool. Also, the SignalP-6.0 server was used to remove signal peptides.

2.4. *In-Silico* Analysis of *B. velezensis* Produced L-ASNase

The physicochemical attributes of L-ASNase were predicted by the ProtParam tool. The 3-D structure was further modeled using the (PS)2-v3 and SWISS-Model servers.

The quality of the generated models was measured by the Ramachandran plot. In the SWISS model, a total of 50 templates were used. The protein secondary structure was further evaluated by employing the SOPMA server. In addition, the potential binding pockets for L-asparagine (searched by the PrankWeb server) and the binding site residues were multiply aligned using the Clustal Omega program. Afterward, the conservation of the functional residues in L-ASNase was deduced using the ConSurf web server. The prediction servers in this study are shown in Table 1.

Table 1: Prediction Servers List

No.	Server	Address	Reference
1	ProtParam	https://web.expasy.org/protparam	Gasteiger *et al*. 2005
2	(PS)2-v3	http://ps2v3.life.nctu.edu.tw	Huang *et al*. 2015
3	SWISS-Model	https://swissmodel.expasy.org/	Guex *et al*. 2009, Bienert *et al*. 2017, Waterhouse *et al*. 2018
4	Ramachandran plot	https://zlab.umassmed.edu/bu/rama/	Lovell *et al*. 2003
5	SOPMA server	https://npsa-prabi.ibcp.fr/cgi-bin/npsa_automat.pl?page=/NPSA/npsa_sopma.html	Geourjon & Deléage 1995
6	Prank web server	https://prankweb.cz/	Krivák & Hoksza 2018, Jendele *et al*. 2019
7	Clustal Omega	https://www.ebi.ac.uk/Tools/msa/clustalo/	Madeira *et al*. 2022
8	ConSurf web	https://consurf.tau.ac.il/	Berezin *et al*. 2004

2.5. Qualitative Measurement of L-ASNase Production

The quality of the produced enzyme and pink zone diameter were measured using the agar well diffusion method (AWDM) and then compared to select the best isolate (Tatari *et al*., 2012).

2.6. Quantitative Assay of L-ASNase Activity

For the quantitative assay of the L-ASNase activity in the selected isolate, 10% inoculum with 0.5 McFarland equivalent concentration was inoculated in 100 ml of L-asparagine broth medium and then incubated at 35ºC for 72 h. The cell-free supernatant containing the enzyme was also obtained by centrifuging the culture broth at 4000 rpm for 10 min and then used for the L-

ASNase assay. For this purpose, 0.5 mL enzyme solution was added to 0.5 mL L-asparagine (0.04 M), 0.5 mL Tris (hydroxymethyl) aminomethane (THAM) hydrochloride (Tris HCl) buffer (0.1 M and pH 8.2), and 0.5 mL distilled water. The mixture was then incubated for 30 min at 37ºC. Afterward, the reaction was stopped by adding 0.5 mL of trichloroacetic acid (TCA, 1.5 M). Blank tubes were also run following the enzyme preparation and the addition of trichloroacetic acid ($C_2HCl_3O_2$). Then, the sample tube was centrifuged for 10 min at room temperature at 10,000 g. Also, 0.1 mL of the previous supernatant and 3.7 mL of distilled water were mixed, and 0.2 mL of Nessler's reagent (K_2HgI_4) was added. The tubes were incubated at room temperature for 15 min, and the absorbance was read at 450 nm. The released NH_3 during the enzyme activity was determined with a standard graph of ammonium sulfate ($(NH_4)_2SO_4$). One unit of the L-ASNase activity was further defined as the amount of enzyme that catalyzed the formation of one micromole of NH_3 per mL in 1 min at 37°C, according to Eq. 1 (Imada *et al*., 1973).

$$\text{Enzyme activity}=\frac{(\mu\text{mol of } NH_3)(2.5)}{(0.1)(30)(0.5)} \quad (1)$$

2.7. Specific Quantitative Colorimetric Assay for of L-ASNase

The Bradford protein assay is known as a colorimetric method to measure protein concentration in biological samples (Bradford, 1976). For the protein assay in this study, a 100 µL enzyme solution and 4.9 mL Bradford's reagent were incubated at room temperature for 5 min. Then, the absorbance was read at 595 nm, and the protein concentration was determined with a standard bovine serum albumin (BSA) graph.

2.8. Optimization of pH and Incubation Time using the One-Factor-at-a-Time (OFAT) Method

The optimum pH level and incubation time were first investigated using the OFAT method (Czitrom, 1999). Five M9 culture media (with a pH of 5.5, 6, 6.5, 7, and 7.5) were also prepared, and incubated at 35°C for three days. Finally, the pink zone diameter was measured.

To investigate the optimal level of the incubation time on the L-ASNase activity, a 100 mL culture medium was prepared without agar and indicator. It was further inoculated (10% of 0.5 McFarland equivalent concentration) and incubated for 24, 48, 72, 96, and 120 h with 100 rpm/min aeration speed. Then, the best incubation time for more enzyme production was achieved by the enzyme activity assay. The effect of pH levels on enzyme activity was investigated using a one-way ANOVA. The enzyme activity was measured at five different pH and incubation time levels. Then, two post-hoc tests (Tukey test and pairwise t-test) were utilized for pairwise mean comparisons of pH and incubation time, respectively.

2.9. Optimization of L-ASNase Production using RSM

The RSM and the CCD were exploited for the optimization of the L-ASNase production (Bezerra et al., 2008). As well a full factorial design was selected, and a total of 30 experiments with three repetitions were developed (Wang & Jee Wu, 1995). The effective variables considered for optimization were temperature (25-45°C), a nitrogen source (0.6-1.4%), a carbon source (0.5-1.5%), and Tween 20 (0.15-0.45%). Minitab software 18 was further used to analyze the results, and lastly, an analysis of variance (ANOVA) of the data was performed (Sthle & Wold, 1989).

3. Results and discussion

3.1. Isolated Microorganism and Molecular Identification

Among 114 isolates, the SE114 strain with a 55 mm pink zone diameter was the best producer of L-ASNase. Accordingly, gene amplification was performed for the strain, and the similarity percentage (NCBI databases) also showed it belonged to *B. velezensis* (MG008635.1) (100%).

L-ASNase is an enzyme that converts L-asparagine into aspartate and ammonia, although L-asparagine is essential for neoplastic cells. Therefore, L-ASNase has been considered as a chemotherapy medicine. Even if some techniques have been thus far developed for enzyme production and purification, they have provided an insufficient quantity of enzymes in limited trials. Against this background, enzyme production by some bacteria can be explored.

3.2. Sequence Retrieval

The specific primers of AAACAATTCATGCCCTTCATTAC (forward) and GTACTCATTGAAATAGGTTTGAATC (reverse) were designed by the Gene Runner tool for L-ASNase gene application using PCR protocol (section sequence retrieval) in *B. velezensis* SE114, and the sequence was determined. The L-ASNase protein sequence, after sequencing and modification, is shown in Supplementary file.

3.3 *In-Silico* Analysis of L-ASNase Produced by *B. velezensis*

The physicochemical properties of the *B. velezensis*-produced L-ASNase were predicted by the ProtParam tool, as depicted in Table 2. The 3-D structures of the monomer and the tetramer were also modeled (Fig 1). As structure analysis is an important step to validate the predicted model of a protein, and the Ramachandran plot is a fundamental tool to visualize the dihedral angles, *w* and *u*, of amino acid residues in a protein for the structural assessment, the Ramachandran plot analysis revealed 295 (97.6%) residues in the favored region, 4 (1.3%) residues in the additional allowed region, and 3 (0.9%) residues in the disallowed one. Therefore, the modeled 3-D structures had good qualities and were assumed to be valid (Fig 2). A signal peptide sequence of 21 amino acids was further determined in the L-ASNase sequence by the SignalP 6.0 server (Fig 3). The presence of signal peptide accordingly indicated that L-ASNase was an extracellular enzyme in *B. velezensis*. The secondary structure was further predicted by the SOPMA server and revealed 30% alpha-helix, 44.57% random coil, 19.43% extended strand, and 6% beta-turn in the L-asparaginase of *B. velezensis* (Fig 4).

Of note, the PrankWeb server is an online resource providing an interface to P2Rank, a state-of-the-art method for ligand binding site prediction. It also allows comparing the location of pockets predicted with highly conserved areas as well as actual ligand binding sites (Jendele *et al*., 2019). In this study, the PrankWeb tool illustrated the binding pocket in the N-terminal domain and ASFL (Fig 5). It also determined that Thr36, Ala47, Tyr50, Glu84, Asp117, Thr116, Met142, Lys189, Thr193, and Thr192 probably had a major role in this interaction in the *B. velezensis*-producing L-ASNase. The multiple sequence alignment of the protein by the Clustal Omega program also showed that all the residues predicted by the Prankweb server were conserved (Supplementary file). Moreover, the ConSurfweb server detected that residues number 36, 50, 116, 117, 189, and 192 were conserved and exposed in the L-ASNase sequence. Accordingly, they probably had a functional role in protein-ligand interaction (Fig 6).

L-ASNase has generally been characterized as a tetrameric protein. According to the Prankweb server results, the enzyme's active site was at the N-terminal domain and the ASFL. Some studies have further revealed that the ASFL plays three principal roles in L-ASNase: first, it makes a cap

to limit access to the active site cavity that helps Thr36 (namely, the primary nucleophilic residue) for presentation to the ligand molecule and forms an oxyanion hole. When the substrate wants to bind to the enzyme, the ASFL is changed, and an oxyanion hole is created. Second, after binding to the ligand, four hydrogen bonds are created in this hole, mediated by water. Thus, the water molecule is a key member of the catalytic procedure. Third, the water molecule accordingly forms the oxyanion hole framework, which is particular from other hydrolases and clearly defines L-ASNases (Lubkowski and Wlodawer, 2021).

It has also been documented that a conserved threonine residue plays a major role in the L-ASNase mechanism and acts as a primary ucleophile for L-asparagine (Palm *et al*., 1996). This nucleophilic residue then attacks L-asparagine and forms an intermediate product. The water molecule also attacks the intermediate product, and the enzyme aspartate NH_3-lyase is created as the final product. However, threonine requires the tyrosine residue adjacently for the L-ASNase activity (Derst *et al*., 1994). Nevertheless, glutamate residue is vital for catalysis since it acts as an activator of tyrosine. Hence, Thr-Tyr-Glu can form a catalytic motif in the L-ASNases (Aghaiypour *et al*., 2001; Ortlund *et al*., 2000).

Furthermore, in a report on binding site prediction for *B. velezensis* L-ASNase, molecular docking revealed an active site in the ASFL and N-terminal domain. Correspondingly, L-ASNase had formed seven hydrogen bonds with the Thr36 residues, Ala47, Tyr50, Asp117, Thr116, Met142, and Thr192 in this interaction, which had a functional role in the L-ASNase and L-asparagine reaction (Hozoorbakhsh *et al*., 2022). As a result, molecular docking and the PrankWeb server agreed with each other in predicting the binding site.

Figure 1: 3-D Structure of *B. velezensis* in the Monomer Form by (PS)2-v3 (right) and Tetramer Form by SWISS-Model (left)

Figure 2: 3-D Structure Quality of L-ASNase Produced by *B. velezensis* which illustrates 97.6% residues are in the favored region.

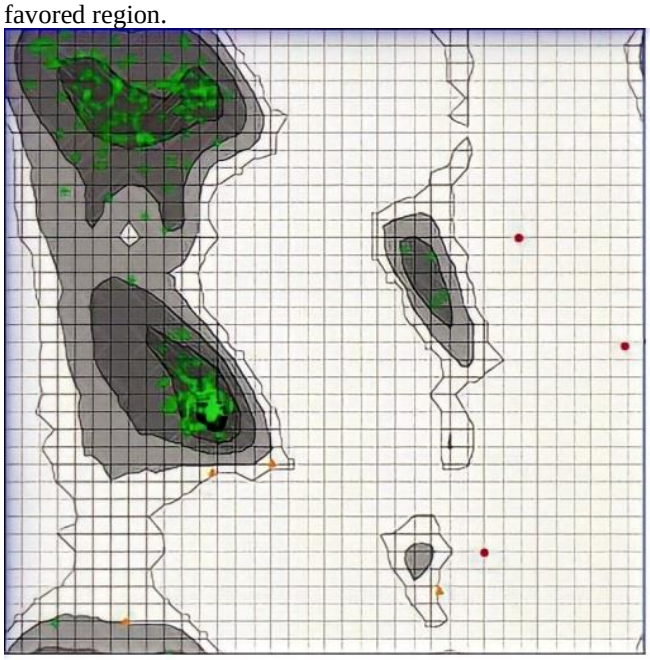

Table 2: Physicochemical Parameters of L-ASNase in *B. velezensis* (SE114)

Total number of atoms	5240			Length (Amino acid)	350
Atomic composition			Namber	Total number of positively charged residues (Arg+Lys)	40
	Carbon	C	1625	Formulation	$C_{1626}H_{2635}N_{451}O_{520}S_8$
	Hydrogen	H	2635		
	Nitogen	N	451		
	Oxygen	O	520		
	Sulfur	S	0		

Amino acid composition	Amino acid	Namber	Percent
	Ala(A)	42	12.00%
	Arg(R)	10	2.90%
	Asn(N)	20	5.70%
	Asp(D)	21	6.00%
	Cys(C)	1	0.30%
	Gln(Q)	11	3.10%
	Glu(E)	15	4.30%
	Gly(G)	29	8.30%
	His(H)	5	1.40%
	Ile(I)	20	5.70%
	Leu(L)	25	7.10%
	Lys(K)	30	8.60%
	Met(M)	7	2.00%
	Phe(F)	7	2.00%
	Pro(P)	17	4.90%
	Ser(S)	22	6.30%
	Thr(T)	32	9.10%
	Trp(W)	0	0.00%
	Tyr(Y)	12	3.40%
	Val(V)	24	6.90%
	Pyl(O)	0	0.00%
	Sec(U)	0	0.00%

Total number of negatively charged residues (Asp+Glu)	36
Molecular weight	37079.00
Theoretical PI	8.83
Instability index	20.52 Stable
Aliphatic index	82.03
GRAVY	- 0.315
Extinction coefficient	17880

Figure 3: Signal peptide sequence of L-ASNase in *B. velezensis* which contains 21 amino acids

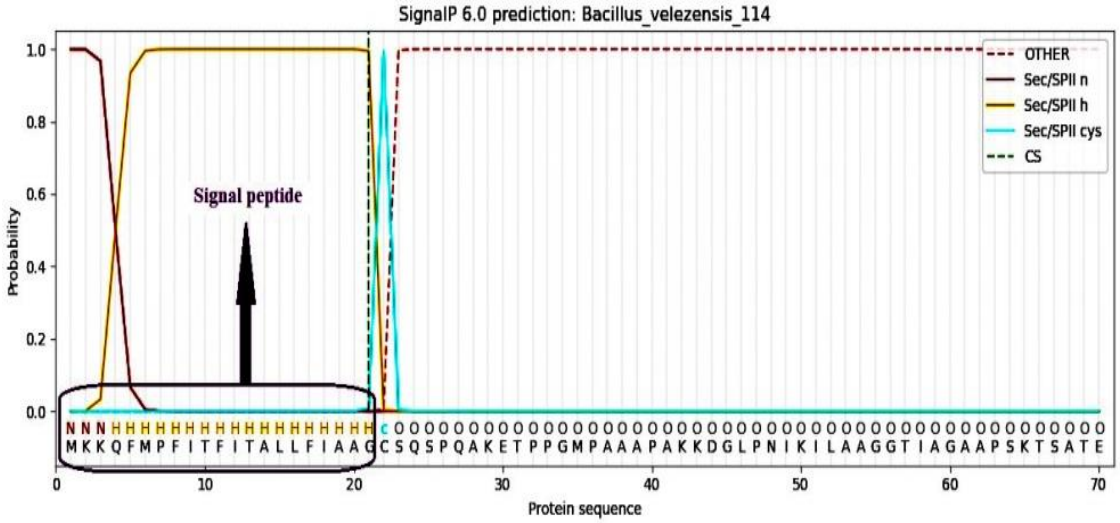

Figure 4: Secondary Structure Analysis of L-ASNase in *B. velezensis* by the SOPMA Server which demonstrates it involves 30% alpha-helix, 44.57% random coil, 19.43% extended strand, and 6% beta-turn.

```
        10        20        30        40        50        60        70
         |         |         |         |         |         |         |
CSQSPQAKETPPGMPAAAPAKKDGLPNIKILAAGGTIAGAAPSKTSATEYTAGAIGVDALIQAVPEIKEV
ccccccccccttccccccccttteeeeeeettceeeccccccccccccccccchhhhhhhhhhhhhh
AHVSGEQVVNIGSQNMNNETLLKLAKRVNKLLKSDDTDGIVITHGTDTLEETAYFLNLTVKSDKPVVVAG
hhhhhhhheeccccccchhhhhhhhhhhhhhhccttcceeeeeccccchhhhhhhheeeccccceeeee
SMRPSTALGADGPSNLYNAVKTAAAPDAKGKGTLVVLNDRIASARYVTKTNTTAADTFKSEEMGYIGTIA
ccccccccccccchhhhhhhhhhctttttceeeeeeccchhhhhhhhcccccccceeeecccccccceeeec
DAVYFNNIMTRKHTKDTDFKIDKLDKLPQVDIIYGYQNDGSYLFEAAVKSGAQGIIFAGPGNGSMSDEAQ
cceeeecccccccccccccccccccccceeeeeeeccccchhhhhhhhttteeeeeeccccccchhhh
KGAVKSVKSGLAVVRSTRTGNGTVTPNREYEKDHLTASNSLNPQKARILLMLALTKTHDPKRIQTYFNEY
hhhhhhhhttceeeeecccccccceeecccccccceeehtccccthhhheehhhhhccccchhhhhhhhhh
```

```
Sequence length :   350
```

```
SOPMA :
   Alpha helix     (Hh) :   105 is  30.00%
   3₁₀ helix       (Gg) :     0 is   0.00%
   Pi helix        (Ii) :     0 is   0.00%
   Beta bridge     (Bb) :     0 is   0.00%
   Extended strand (Ee) :    68 is  19.43%
   Beta turn       (Tt) :    21 is   6.00%
   Bend region     (Ss) :     0 is   0.00%
   Random coil     (Cc) :   156 is  44.57%
   Ambiguous states (?)  :     0 is   0.00%
   Other states          :     0 is   0.00%
```

Figure 5: Predicted Binding Site of L-ASNase in *B. velezensis* at the N-terminal domain and the ASFL by the PrankWeb Server, in Blue

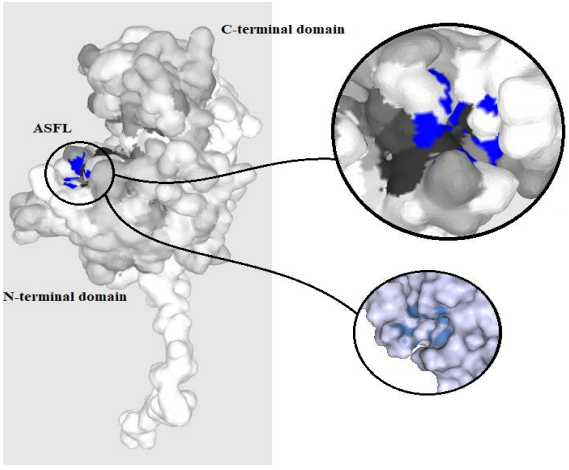

Figure 6: Prediction of High Conserved and Exposed Residues of L-ASNase in *B. velezensis* by the ConSurf Web Server (residues number 36, 50, 116, 117, 189, and 192)

3.4 Optimization of pH and Incubation Time using the OFAT Method

To investigate the effect of pH on L-ASNase production, the enzyme qualitative assay was evaluated at the pH of 5.5, 6, 6.5, 7, and 7.5, and the results revealed that *B. velezensis* had the most L-ASNase production at pH 6.5 (Fig 7). A one-way ANOVA revealed that there was a statistically significant difference in enzyme activity between five pH levels (F-value of 20.32 and P-value <0.01). A post-doc Tukey`s HSD test showed that the enzyme activity at pH 6-6.5 (P-

Figure 7: Optimization of pH for L-ASNase Production using OFAT Method reveales that the most L-ASNase is produced at pH 6.5

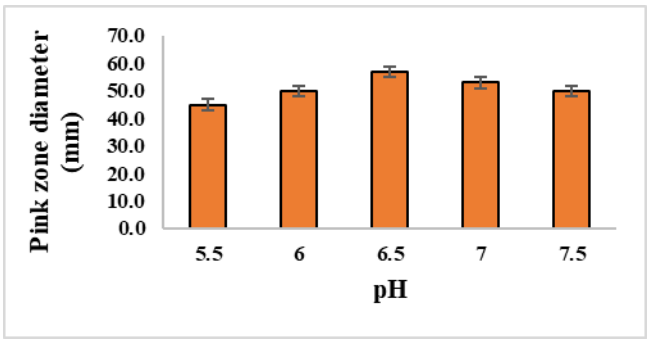

values of 0.002) was significantly higher than at pH 5.5-6 (P-value of 0.04). Also, there was no significant difference in enzyme activity at pH 6.5-7 and 7-7.5 (P-value of 0.09 and 0.19). Finally, the result of the ANOVA test supported the hypothesis that pH levels affect enzyme activity.

Quantitative assay for enzyme activity and specific activity also established that the best incubation time for the L-ASNase production was 72 h with 3.02 and 5.8 U/mL, respectively (Fig 8). In addition, a one-way ANOVA revealed that there was a statistically significant difference in enzyme activity between the nine incubation times (F-value of 148.637 and P-value <0.01). A post-doc pairwise t-test illustrated that the enzyme activity at 32-72 hours (P-values of 0.004) was significantly higher than at other incubation times. Also, there was no significant difference in enzyme activity at 6, 12, 24, 48, 120 hours. Consequently, the result of the ANOVA test demonstrated that incubation time affects enzyme activity.

Figure 8: OFAT Optimization for Incubation Time investigates that the best incubation time for the L-ASNase production is 72 h with 3.02 and 5.8 U/mL, respectively.

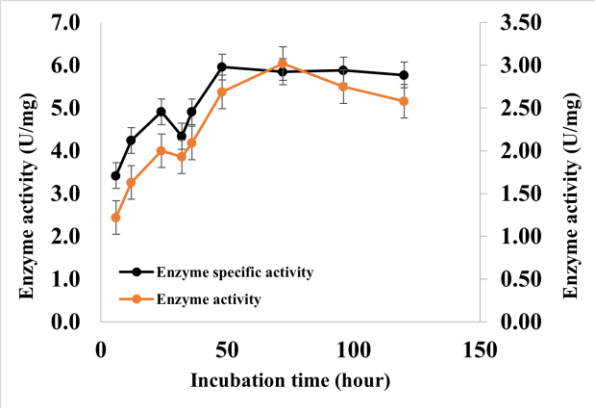

In a report on the L-ASNase optimization for B. velezensis, the L-ASNase production was accordingly optimized using the OFAT method in 2019, illustrating that 72 h and pH 6.5 were the best for enzyme activity. In addition, they found that the significant productivity of the enzyme occurred at 72 h, pH 6.5, 37°C, and 100 rpm. Also, different carbon and nitrogen sources evaluated for L-ASNase production demonstrated that glucose and L-asparagine were suitable (Mostafa et al., 2019). In this line, glucose and L-asparagine were selected as the carbon and nitrogen sources in the present study, and the L-ASNase production by *B. velezensis* was optimized by the OFAT method and the RSM

3.5 L-ASNase Production Optimization using RSM

The influence of temperature, L-asparagine (as a nitrogen source), glucose (as a carbon source), and Tween 20 on L-ASNase production during 30 runs was evaluated by the RSM (Table 3). Enzyme activities were also obtained from 1.49 to 6.51 U/mL. In this respect, run number 24 with 0.45% Tween 20 concentration, 1.5% glucose concentration, 45°C temperature, and 1.4% L-asparagine concentration had the highest amount of enzyme activity with the value of 6.51 U/mL.

Figure 9: Pareto Chart of Standardized Effects illustrates tween 20, glucose, temperature, and L-asparagine are the most effective factors, respectively (the response is the enzyme activity, U/mL)

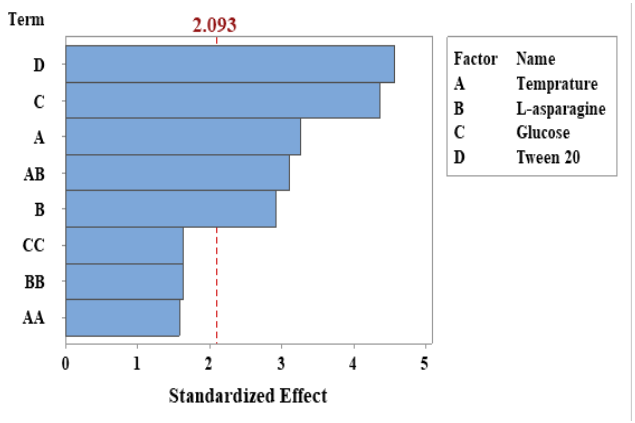

The statistical analysis also demonstrated that the model with an F-value of 8.88 and a P-value of was significant (Table 4). All factors were additionally significant (P-values<0.05). The interaction between temperature and L-asparagine was also significant, with a P-value of 0.006. The Pareto chart in (Fig 9) illustrates Tween 20, glucose, temperature, and L-asparagine as the most effective factors. Moreover, normal

probability showed that the data were normal and random (Fig 10). The regression analysis software results presented the relationship between the variables and the enzyme activity (as displayed in Equation 2).

Enzyme activity (U/mL) = -1.18
+ 0.0659 Temperature - 0.85 L-asparagine
+ 2.658 Glucose
+ 3.840 Tween 20- (2)
0.00209 Temperature*Temperature- 1.232 L-asparagine*L-asparagine - 0.788 Glucose*Glucose
+ 0.1210 Temperature*L-asparagine

Based on this study's statistical approach using RSM optimization, the highest enzyme activity, with a value of 7.11 U/mL, was obtained at 0.6% Tween 20 concentration, 1.7% glucose concentration, 55°C temperature, and 1.8% L-asparagine concentration (Fig 11). The 3-D response surface graph also showed that the interaction between L-asparagine and temperature was significant (Fig 12). More observations further showed a relationship between L-asparagine and temperature. L-asparagine also acted as an inducer and source of nitrogen. The L-ASNase activity was thus enhanced by increasing temperature up to 55°C in the L-asparagine concentration of 1 and 1.4%, but there was no similar effect at 0.6% L-asparagine concentration (Fig 13).

Figure 10: Normal Probability Plot shows that the data is normal and random (the response is the enzyme activity, U/mL)

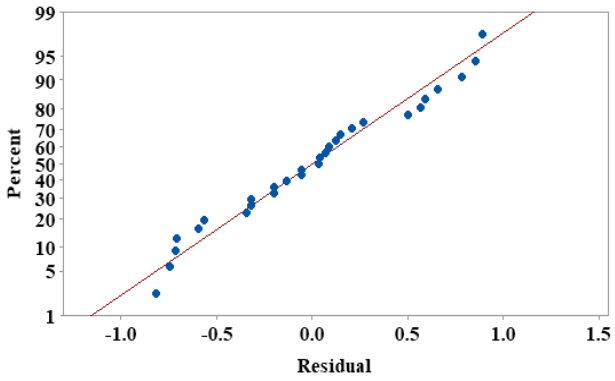

Moreover, glucose provided a positive effect to enhance L-ASNase biosynthesis, as described in another study. *B. licheniformis* enzyme productivity was improved by gamma irradiation and then optimized by the RSM experimental design (viz., the Box-Behnken central composite design). Besides, the optimum conditions for the maximum L-ASNase production by the improved mutant were 39.57°C, 7.39 pH, 20.74 h, 196.40 rpm, 0.5% glucose, 0.1% ammonium chloride (NH_4Cl), and 10 mM magnesium sulphate (MgSO4). Both *B. velezensis* and *B. licheniformis* also had high activity in the close glucose concentration of 1.6 and 0.5, respectively (Abdelrazek *et al*. 2019).

Figure 11: Main Effect Plot for Enzyme Activity (U/mL) demonstrates the highest enzyme activity, with a value of 7.11 U/mL, obtains at 0.6% Tween 20 concentration, 1.7% glucose concentration, 55°C temperature, and 1.8% L-asparagine concentration.

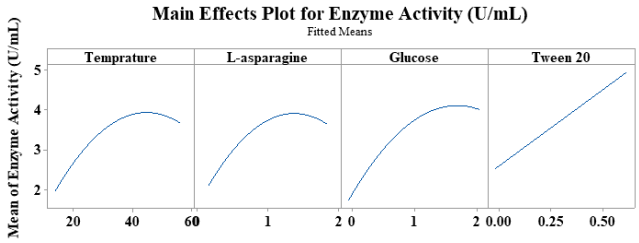

Figure 12: 3-D Response Graph Representing the Interaction between L-asparagine and Temperature which is significant.

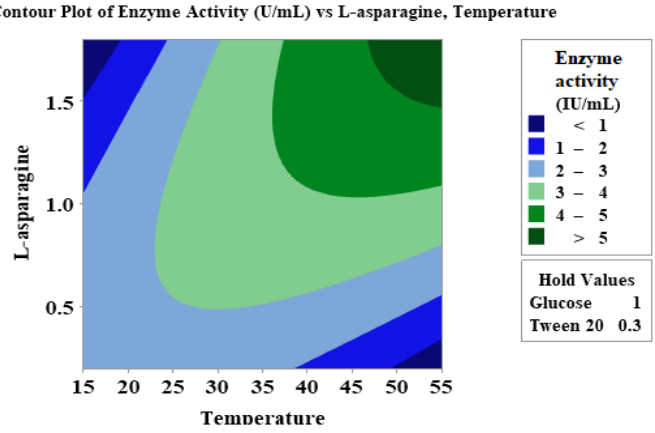

Elshafei and El-Ghonemy (2015) also evaluated the effect of 0.1% Tween 20, 60, and 80 on L-ASNase production using filamentous fungi and indicated that surfactants, such as Tween 20, could increase the L-ASNase production by 1.19 fold due to promoting the entrance of some compounds into cells. Therefore, Tween 20 was selected as a factor in optimization in this study, and both that and this study showed that Tween 20 had a profound effect on enzyme activity. The L-ASNase production in *B. australimaris* using the Box-Behnken design has also been evaluated, and the optimal variables were achieved at 2.44% L-asparagine concentration, pH 6.77, 1.57% inoculum size, and 33.5°C temperature (Chakravarty *et al*., 2021). Moreover, another study found that both *B. velezensis* and *B. australimaris* have more activity in the same pH (with values of 6.5 and 6.7) and L-asparagine concentration (with values of 1.8 and 2.44%), respectively. In contrast, the optimum temperature was very different, with a value of 55°C for *B. velezensis* and 33.5°C for *B. australimaris*, because *B. australimaris* was mesophilic while *B. velezensis* was thermophilic (Elegbeleye & Buys, 2020; Liu *et al*., 2016).

Several reports have further determined that *B. velezensis* is resistant to high temperatures and grows from 6 to 55°C. It also produces biofilm and heat-resistant enzymes (Elegbeleye & Buys, 2020). For example, it has been established that *B. velezensis* could have thermostable xylanase and produce the highest amount of enzyme at 50°C (Ghosh *et al*., 2021). *B. velezensis* was also found to produce thermostable amylase, with the highest activity at 50°C (Hu *et al*., 2022). In addition, the thermophilic proteins had more alanine than the psychrophilic ones (Vieille & Zeikus, 2001).

The prediction of the physicochemical parameters of L-ASNase in *B. velezensis* using the ProtParam server accordingly revealed that *B. velezensis* had 12% alanine, see Table 2. Moreover, the thermophilic proteins had more hydrophobic residues in the core as well as more hydrogen and salt bonds on the surface (Schweizer & Mueller, 2014). Additionally, the analysis of the interactions between L-asparagine and temperature showed two approaches for increasing enzyme activity. Choosing a 35°C temperature and a higher concentration of L-asparagine (e.g., 2.5%) or selecting a 55°C temperature and a lower concentration of L-asparagine (e.g., 1.8%), both approaches could thus accelerate the enzyme activity to a significant extent (Fig 13).

Verification of the Model: In order to determine the accuracy of the model and to verify the result, an experiment under the optimal conditions obtained was performed and compared with the predicted data. The measured L-asparaginase activity obtained was 7.29 U/mL, close to the predicted 7.11 U/mL, revealing a high degree of accuracy. The model's verification revealed a degree of accuracy of more than 97.5%, indicating the model validation under the tested conditions.

Figure 13: Interaction plot for enzyme activity (U/mL) between L-asparagine and temperature.The L-ASNase activity was thus enhanced by increasing temperature up to 55°C in the L-asparagine concentration of 1 and 1.4%, but there was no similar effect at 0.6% L-asparagine concentration.

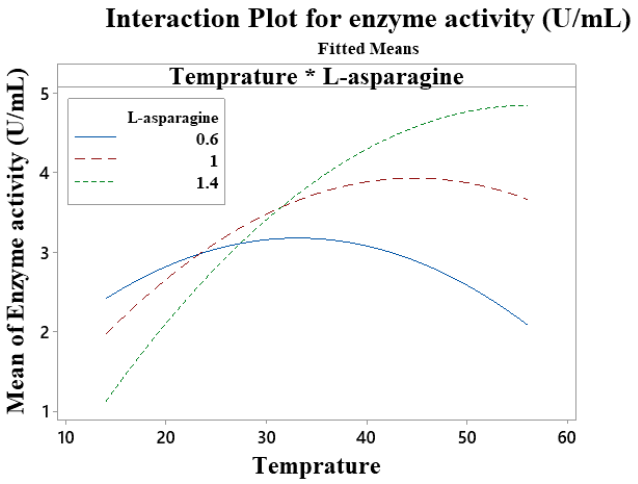

.

Table 3: Experimental Plan Based on a Central Composite Design for L-ASNase Production Optimization using Minitab Software 18

RunOrder	PtType	Blocks	Temperature	L-asn	Glucose	Tween 20	Enzyme activity observed) U/mL (	Enzyme activity predicted)U/mL(	Specific enzyme activity)U/mg(
1	-1	2	35	1	2	0.3	2.92	4.04	6.55
2	0	2	35	1	1	0.3	3.17	3.74	11.91
4	-1	2	35	0.2	1	0.3	1.74	2.22	3.99
5	-1	2	35	1	1	0	2.64	2.59	18.75
6	-1	2	35	1	1	0.6	3.56	4.89	6.66
7	-1	2	55	1	1	0.3	2.49	3.72	11.12
8	-1	2	35	1.8	1	0.3	3.32	3.69	7.89
9	-1	2	15	1	1	0.3	3.49	2.09	7.79
10	-1	2	35	1	0	0.3	2.14	1.87	4.73
11	0	1	35	1	1	0.3	3.17	3.74	8.55
12	1	1	45	1.4	0.5	0.45	5.52	4.43	9.34
13	1	1	25	0.6	1.5	0.45	3.54	3.96	6.61
14	1	1	25	0.6	0.5	0.45	2.44	2.88	5.66
15	0	1	35	1	1	0.3	3.09	3.74	8.04
16	1	1	45	0.6	1.5	0.15	3.28	2.66	10.52
17	0	1	35	1	1	0.3	3.88	3.74	13.49
18	1	1	25	1.4	0.5	0.15	1.68	1.50	6.66
19	1	1	45	0.6	0.5	0.15	2.34	1.57	7.18
20	1	1	25	0.6	0.5	0.15	1.49	1.73	5.23
21	1	1	45	0.6	0.5	0.45	2.66	2.73	4.49
22	1	1	25	1.4	1.5	0.15	2.88	2.58	11.29
23	1	1	45	1.4	0.5	0.15	3.46	3.28	11.27
24	1	1	45	1.4	1.5	0.45	6.51	5.51	10.47
25	1	1	25	1.4	1.5	0.45	4.44	3.73	8.41
26	1	1	25	0.6	1.5	0.15	2.97	2.81	11.10
27	1	1	45	1.4	1.5	0.15	4.66	4.36	14.02
28	0	1	35	1	1	0.3	3.26	3.74	8.61
29	1	1	45	0.6	1.5	0.45	5.16	3.81	8.92
30	1	1	25	1.4	0.5	0.45	2.44	2.65	4.23

Table 4: ANOVA for Optimization demonstrates that the model with an F-value of 8.88 and a P-value of 0.000 was significant

Source	DF	Adj SS	Adj MS	F-Value	P-Value
Model	9	29.4030	3.2670	8.88	0.000
Blocks	1	5.2401	5.2401	14.24	0.001
Linear	4	22.1210	5.5303	15.03	0.000
Temperature	1	3.9285	3.9285	10.68	0.004
L-asparagine	1	3.1504	3.1504	8.56	0.009
Glucose	1	7.0092	7.0092	19.05	0.000
Tween 20	1	7.7080	7.7080	20.95	0.000
Square	3	1.9967	0.6656	1.81	0.180
Temperature*Temperature	1	0.9254	0.9254	2.52	0.129
L-asparagine*L-asparagine	1	0.9912	0.9912	2.69	0.117
Glucose*Glucose	1	0.9912	0.9912	2.69	0.117
2-way interaction	1	3.5710	3.5710	9.71	0.006
Temperature*L-asparagine	1	3.5710	3.5710	9.71	0.006
Error	19	6.9897	0.3679		
Lack-of-fit	15	6.5747	0.4383	4.23	0.087
Pure error	4	0.4149	0.1037		
Total	28	36.3926			

4. Conclusion

This study concluded that a combination of the RSM and the CCD was effective in selecting the significant factors in the optimization of the bioprocess for L-ASNase production by *B. velezensis* SE114. Moreover, Tween 20, glucose, temperature, and L-asparagine were among the significant variables in the L-ASNase production. In addition, temperature and L-asparagine had noteworthy interactions. The in-silico studies correspondingly predicted the residues of Thr36, Ala47, Tyr50, Glu84, Thr116, Asp117, Met142, Lys189, Thr192, and Thr193 at the binding site, and they were conserved. In this way, they probably had a functional role in the protein-ligand interaction of L-ASNase of *B. velezensis*.

Author contribution:

All authors contributed to the study's conception and design. Material preparation, data collection, and analysis were performed by Fereshteh Hozoorbakhsh. The first draft of the manuscript was written by Fereshteh Hozoorbakhsh, and all authors commented on and edited subsequent versions. All authors read and approved the final manuscript.

Conflict of interest

The authors declare no conflict of interest.

Appendix A. Supplementary data file

Acknowledgment

This research was carried out with the financial support of the Scientific and Industrial Research Organization of Iran and in the graduate education field of that organization, the Agriculture Unit.

Ethical approval

This article does not contain any studies with human participants or animals performed by any of the authors.

Open access

References

[1] Abdelrazek, N. A., Elkhatib, W. F., Raafat, M. M., & Aboulwafa, M. M. (2019). Experimental and bioinformatics study for production of L-asparaginase from *Bacillus licheniformis*: a promising enzyme for medical application. *Amb Express*, *9*(1), 39. https://doi.org/10.1186/s13568-019-0751-3

[2] Aghaiypour, K., Wlodawer, A., & Lubkowski, J. (2001). Do bacterial L-asparaginases utilize a catalytic triad Thr-Tyr-Glu?. *Biochimica et Biophysica Acta (BBA)-Protein Structure and Molecular Enzymology*, *1550*(2), 117-128. https://doi.org/10.1016/S0167-4838(01)00270-9

[3] Berezin, C., Glaser, F., Rosenberg, J., Paz, I., Pupko, T., Fariselli, P., ... & Ben-Tal, N. (2004). ConSeq: the identification of functionally and structurally important residues in protein sequences. *Bioinformatics*, *20*(8), 1322-1324. https://doi.org/10.1093/bioinformatics/bth070

[4] Bezerra, M. A., Santelli, R. E., Oliveira, E. P., Villar, L. S., & Escaleira, L. A. (2008). Response surface methodology (RSM) as a tool for optimization in analytical chemistry. *Talanta*, *76*(5), 965-977.

[5] Bienert, S., Waterhouse, A., De Beer, T. A., Tauriello, G., Studer, G., Bordoli, L., & Schwede, T. (2017). The SWISS-MODEL Repository—new features and functionality. *Nucleic Acids Research*, *45*(D1), D313-D319. https://doi.org/10.1093/nar/gkw1132

[6] Bradford, M. M. (1976). A rapid and sensitive method for the quantitation of microgram quantities of protein utilizing the principle of protein-dye binding. *Analytical Biochemistry*, *72*(1-2), 248-254. https://doi.org/10.1006/abio.1976.9999

[7] Chakravarty, N., Singh, J., & Singh, R. P. (2021). A potential type-II L-asparaginase from marine isolate *Bacillus australimaris* NJB19: statistical optimization, in silico analysis and structural modeling. *International Journal of Biological Macromolecules*, *174*, 527-539. https://doi.org/10.1016/j.ijbiomac.2021.01.130

[8] Czitrom, V. (1999). One-factor-at-a-time versus designed experiments. *The American Statistician*, *53*(2), 126-131. https://doi.org/10.1080/00031305.1999.10474445

[9] Darvishi, F., Jahanafrooz, Z., & Mokhtarzadeh, A. (2022). Microbial L-asparaginase as a promising enzyme for treatment of various cancers. *Applied Microbiology and*

Biotechnology, *106*(17), 5335-5347. https://doi.org/10.1007/s00253-022-12086-8
[10] Derst, C., Wehner, A., Specht, V., & Röhm, K. H. (1994). States and functions of tyrosine residues in Escherichia coli asparaginase II. *European Journal of Biochemistry*, *224*(2), 533-540. https://doi.org/10.1111/j.1432-1033.1994.00533.x
[11] Elegbeleye, J. A., & Buys, E. M. (2020). Molecular characterization and biofilm formation potential of *Bacillus subtilis* and *Bacillus velezensis* in extended shelf-life milk processing line. *Journal of Dairy Science*, *103*(6), 4991-5002. https://doi.org/10.3168/jds.2019-17919
[12] Elshafei, A. M., & El-Ghonemy, D. H. (2015). Screening and media optimization for enhancing L-asparaginase production, an anticancer agent, from different filamentous fungi in solid state fermentation. *British Biotechnology Journal*, *9*(3), 1-15. https://doi.org/10.9734/bbj/2015/19728
[13] Erva, R. R., Venkateswarulu, T. C., & Pagala, B. (2018). Multi level statistical optimization of l-asparaginase from *Bacillus subtilis* VUVD001. *3 Biotech*, *8*(1), 24. https://doi.org/10.1007/s13205-017-1020-2
[14] Gasteiger, E., Hoogland, C., Gattiker, A., Duvaud, S. E., Wilkins, M. R., Appel, R. D., & Bairoch, A. (2005). *Protein Identification and Analysis Tools on the ExPASy Server* (pp. 571-607). Humana press.
[15] Geourjon, C., & Deleage, G. (1995). SOPMA: significant improvements in protein secondary structure prediction by consensus prediction from multiple alignments. *Bioinformatics*, *11*(6), 681-684. https://doi.org/10.1093/bioinformatics/11.6.681
[16] Ghaderi, F., & Ghezelbash, G. R. (2017). Isolation and optimization of glutaminase-free L-asparaginase enzyme producing *Serratia marcescens* isolated from natural sources. *Journal of Microbial World*, *10*(1), 49-58.
[17] Ghiasian, M., Akhavan, S. A., Amoozegar, M. A., Saadatmand, S., & Shavandi, M. (2017). Bacterial diversity determination using culture-dependent and culture-independent methods. *Global J. Environ. Sci. Manage*, *3*(2), 153-164. https://doi.org/10.22034/gjesm.2017.03.02.004
[18] Ghosh, A., Chandra, A., Dhar, A., Shukla, P., & Baishya, D. (2021). Multi-efficient thermostable endoxylanase from *Bacillus velezensis* AG20 and its production of xylooligosaccharides as efficient prebiotics with anticancer activity. *Process Biochemistry*, *109*, 59-71. https://doi.org/10.1016/j.procbio.2021.06.011
[19] Guex, N., Peitsch, M. C., & Schwede, T. (2009). Automated comparative protein structure modeling with SWISS-MODEL and Swiss-PdbViewer: A historical perspective. *Electrophoresis*, *30*(S1), S162-S173. https://doi.org/10.1002/elps.200900140
[20] Hozoorbakhsh, F., Ghiasian, M., Ghandehari, F., Emami-Karvani, Z., & Khademi Dehkordi, M. (2022). An immunoinformatic approach employing molecular docking and molecular dynamics simulation for evaluation of l-asparaginase produced by *Bacillus velezensis*. *Journal of Biomolecular Structure and Dynamics*, 1-15. https://doi.org/10.1080/07391102.2022.2139765
[21] Hu, Q., Wu, Q., Dai, B., Cui, J., Khalid, A., Li, Y., & Wang, Z. (2022). Fermentation optimization and amylase activity of endophytic *Bacillus velezensis* D1 isolated from corn seeds. *Journal of Applied Microbiology*, *132*(5), 3640-3649. https://doi.org/10.1111/jam.15503
[22] Huang, T. T., Hwang, J. K., Chen, C. H., Chu, C. S., Lee, C. W., & Chen, C. C. (2015). 2: protein structure prediction server version 3.0. *Nucleic Acids Research*, *43*(W1), W338-W342. https://doi.org/10.1093/nar/gkv454
[23] Imada, A., Igarasi, S., Nakahama, K., & Isono, M. (1973). Asparaginase and glutaminase activities of micro-organisms. *Microbiology*, *76*(1), 85-99. https://doi.org/10.1099/00221287-76-1-85
[24] Jendele, L., Krivak, R., Skoda, P., Novotny, M., & Hoksza, D. (2019). PrankWeb: a web server for ligand binding site prediction and visualization. *Nucleic Acids Research*, *47*(W1), W345-W349. https://doi.org/10.1093/nar/gkz424
[25] Krivák, R., & Hoksza, D. (2018). P2Rank: machine learning based tool for rapid and accurate prediction of ligand binding sites from protein structure. *Journal of Cheminformatics*, *10*, 1-12. https://doi.org/10.1186/s13321-018-0285-8
[26] Liu, Y., Lai, Q., Du, J., & Shao, Z. (2016). *Bacillus zhangzhouensis* sp. nov. and *Bacillus australimaris* sp. nov. *International Journal of Systematic and Evolutionary Microbiology*, *66*(3), 1193-1199. https://doi.org/10.1099/ijsem.0.000856
[27] Lovell, S. C., Davis, I. W., Arendall III, W. B., De Bakker, P. I., Word, J. M., Prisant, M. G., ... & Richardson, D. C. (2003). Structure validation by Cα geometry: ϕ, ψ and Cβ deviation. *Proteins: Structure, Function, and Bioinformatics*, *50*(3), 437-450. https://doi.org/10.1002/prot.10286
[28] Lubkowski, J., & Wlodawer, A. (2021). Structural and biochemical properties of L-asparaginase. *The FEBS Journal*, *288*(14), 4183-4209.
[29] Madeira, F., Pearce, M., Tivey, A. R., Basutkar, P., Lee, J., Edbali, O., ... & Lopez, R. (2022). Search and sequence analysis tools services from EMBL-EBI in 2022. *Nucleic Acids Research*, *50*(W1), W276-W279. https://doi.org/10.1093/nar/gkac240
[30] Mangamuri, U., Vijayalakshmi, M., Ganduri, V. S. R. K., Rajulapati, S. B., & Poda, S. (2017). Extracellular L-asparaginase from *Streptomyces labedae* VSM-6: Isolation, production and optimization of culture conditions using RSM. *Pharmacognosy Journal*, *9*(6). https://doi.org/10.5530/pj.2017.6.146
[31] Mohammadi-Sichani, M. E., Mazaheri Assadi, M., Farazmand, A., Kianirad, M., Ahadi, A. M., & Hadian-Ghahderijani, H. (2019). Ability of Agaricus bisporus, Pleurotus ostreatus and Ganoderma lucidum compost in biodegradation of petroleum hydrocarbon-contaminated soil. *International Journal of Environmental Science and*

Technology, *16*, 2313-2320. https://doi.org/10.1007/s13762-017-1636-0

[32] Mostafa, Y., Alrumman, S., Alamri, S., Hashem, M., Al-izran, K., Alfaifi, M., ... & Taha, T. (2019). Enhanced production of glutaminase-free L-asparaginase by marine *Bacillus velezensis* and cytotoxic activity against breast cancer cell lines. *Electronic Journal of Biotechnology*, *42*, 6-15. https://doi.org/10.1016/j.ejbt.2019.10.001

[33] Ortlund, E., Lacount, M. W., Lewinski, K., & Lebioda, L. (2000). Reactions of Pseudomonas 7A glutaminase-asparaginase with diazo analogues of glutamine and asparagine result in unexpected covalent inhibitions and suggests an unusual catalytic triad Thr-Tyr-Glu. *Biochemistry*, *39*(6), 1199-1204. https://doi.org/10.1021/bi991797d

[34] Palm, G. J., Lubkowski, J., Derst, C., Schleper, S., Röhm, K. H., & Wlodawer, A. (1996). A covalently bound catalytic intermediate in Escherichia coli asparaginase: Crystal structure of a Thr-89-Val mutant. *FEBS Letters*, *390*(2), 211-216. https://doi.org/10.1016/0014-5793(96)00660-6

[35] Parmar, F. A., Patel, J. N., & Upasani, V. N. (2021). Screening of microorganisms for production of therapeutic enzymes. *Screening*, *3*(6), 39.

[36] Rabbee, M. F., Ali, M. S., Choi, J., Hwang, B. S., Jeong, S. C., & Baek, K. H. (2019). *Bacillus velezensis*: a valuable member of bioactive molecules within plant microbiomes. *Molecules*, *24*(6), 1046. https://doi.org/10.3390/molecules24061046

[37] Rahnamay Roodposhti, F., Asadpour, L., Shahriarinour, M., Rasti, B., & Gharaghani, S. (2023). Optimization of L-asparaginase production using native soil-isolated *Bacillus* sp. and evaluation of its anticancer activity. *Journal of Microbial World*, *15*(4), 259-270. 10.30495/jmw.2022.1967544.2035

[38] Schweizer, L., & Mueller, L. (2014). Protein conformational dynamics and signaling in evolution and pathophysiology. In *Biased Signaling in Physiology, Pharmacology and Therapeutics* (pp. 209-249). Academic Press. https://doi.org/10.1016/B978-0-12-411460-9.00007-0

[39] St, L., & Wold, S. (1989). Analysis of variance (ANOVA). *Chemometrics and Intelligent Laboratory Systems*, *6*(4), 259-272. https://doi.org/10.1016/0169-7439(89)80095-4

[40] Tatari, M., Ghazvini, R. F., Etemadi, N., Ahadi, A. M., & Mousavi, A. (2012). Analysis of antioxidant enzymes activity, lipid peroxidation and proline content of *Agropyron desertorum* under drought stress. *Biology and Environment*, *3*(1), 9-24.

[41] Venil, C. K., Nanthakumar, K., Karthikeyan, K., & Lakshmanaperumalsamy, P. (2009). Production of l-asparaginase by Serratia marcescens SB08: optimization by response surface methodology. *Iranian Journal of Biotechnology*, *7*(1), 10-18.

[42] Vieille, C., & Zeikus, G. J. (2001). Hyperthermophilic enzymes: sources, uses, and molecular mechanisms for thermostability. *Microbiology and Molecular Biology Reviews*, *65*(1), 1-43. https://doi.org/10.1128/mmbr.65.1.1-43.2001

[43] Wang, J. C., & Wu, C. J. (1995). A hidden projection property of Plackett-Burman and related designs. *Statistica Sinica*, 235-250.

[44] Waterhouse, A., Bertoni, M., Bienert, S., Studer, G., Tauriello, G., Gumienny, R., ... & Schwede, T. (2018). SWISS-MODEL: homology modelling of protein structures and complexes. *Nucleic Acids Research*, *46*(W1), W296-W303. https://doi.org/10.1093/nar/gky427